

Halo Assembly Bias in the Quasi-linear Regime

Jose Ariel Keselman^{*} and Adi Nusser

Physics department, IIT, Technion city, Haifa, Israel

11 March 2019

ABSTRACT

We address the question of whether or not assembly bias arises in the absence of highly non-linear effects such as tidal stripping of halos near larger mass concentrations. Therefore, we use a simplified dynamical scheme where these effects are not modeled. We choose the punctuated Zel’dovich (PZ) approximation, which prevents orbit mixing by coalescing particles coming within a critical distance of each other. A numerical implementation of this approximation is fast, allowing us to run a large number of simulations to study assembly bias. We measure an assembly bias from 60 PZ simulations, each with 512^3 cold particles in a $128h^{-1}\text{Mpc}$ cubic box. The assembly bias estimated from the correlation functions at separations of $\lesssim 5h^{-1}\text{Mpc}$ for objects (halos) at $z = 0$ is comparable to that obtained in full N-body simulations. For masses $4 \times 10^{11}h^{-1}M_{\odot}$ the “oldest” 10% haloes are 3-5 times more correlated than the “youngest” 10%. The bias weakens with increasing mass, also in agreement with full N-body simulations. We find that that halo ages are correlated with the dimensionality of the surrounding linear structures as measured by the parameter $(\lambda_1 + \lambda_2 + \lambda_3)/(\lambda_1^2 + \lambda_2^2 + \lambda_3^2)^{1/2}$ where λ_i are proportional to the eigenvalues of the velocity deformation tensor. Our results suggest that assembly bias may already be encoded in the early stages of the evolution.

Key words: methods: N-body simulations – methods: numerical –dark matter – galaxies: haloes – galaxies: clusters: general

1 INTRODUCTION

A fundamental question in cosmology is the relation between the galaxy distribution and the underlying density field of the gravitationally dominant dark matter. According to the standard paradigm of structure formation, galaxies are harbored in stable virialized objects (halos) made of dark matter particles. An assumption that has been often made is that the clustering properties of halos depend on their mass alone. Although the assumption seems over-simplistic given the complexity of the hierarchical process of halo formation, it is sustained by the excursion set theory (Bond et al. 1991; Lacey & Cole 1993; Mo & White 1996) and by results of N-simulations of intermediate resolution (Lemson & Kauffmann 1999; Percival et al. 2003). Only recently Gao, Springel & White (2005) used a simulation of exceptionally large dynamical range (the millennium simulation) to show that the clustering of halos depend also on their age, which is defined as the time since a halo acquired half of its current mass. They have found, that the “oldest” 10% of the halos with mass $10^{11}h^{-1}M_{\odot}$ are more than 5 times more correlated than the “youngest” 10% halos of the same mass. This assembly bias has been confirmed by Harker et

al. (2006) using marked correlation functions on the same simulation, and by Wechsler et al. (2006) and Jing & Mo (2006) using independent simulations.

We still lack a completely satisfactory explanation for the origin of assembly bias. Simple arguments based on the spherical collapse model applied to narrow and broad initial density peaks do predict an assembly bias, but with younger halos being more clustered than older ones (e.g. Sheth & Tormen 2004). This trend of the bias is opposite to what is seen in simulations. Tidal stripping has been also invoked as a possible mechanism (e.g. Diemand, Kuhlen & Madau 2007; Wang, Mo & Jing 2006). Because of mass stripping by the tidal gravitational field of the large mass concentration, nearby halos would have been of higher mass in a different environment. Therefore, these halos would have earlier formation times and would be more biased than halos of the same mass in the field. However, the extent of this effect is difficult to assess. Here we examine whether the bias can, at least partially, arise in the quasi-linear evolution. In order to eliminate highly non-linear effects such as tidal stripping, we adopt approximate methods based on the Zel’dovich approximation (Zel’dovich 1970) where particles move on straight lines independent of the motion of other particles. The Zel’dovich approximation is an analytic solution to planar cosmological perturbations up to the stage

^{*} Email: kari@tx.technion.ac.il

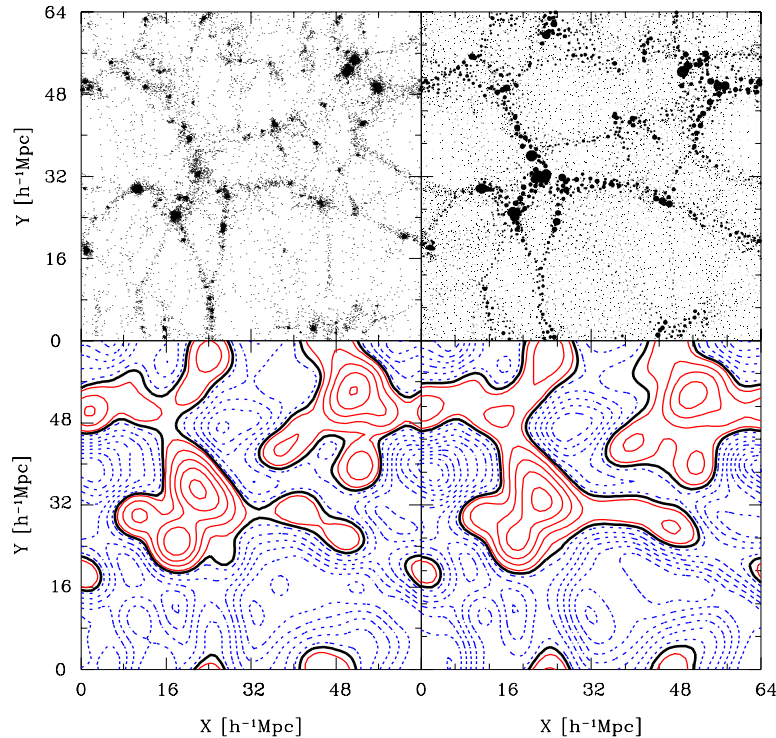


Figure 1. A visual comparison between results of the PZ approximation (right) and a PM N-body code (left) run with the same initial conditions for 256^3 particles in a box of $64\text{Mpc}h^{-1}$ on the side. *Top:* particle (object for PZ) distributions in a slice of $3.2\text{Mpc}h^{-1}$ in thickness (for the PM only a random subset of all the particles is shown). For the PZ, each object is represented as a filled circle with radius proportional to the mass. *Bottom:* contours maps of $\log_{10}(\text{density})$ in the same slice. The density fields are smoothed with a Gaussian window of a width of $1.125\text{Mpc}h^{-1}$. The thin solid and dashed lines are density contours above and below the mean, respectively. Thick solid lines indicate mean density contours. The contour spacing is 0.18.

where multi-streaming appears. For three dimensional perturbations, the approximation is a reasonable description of quasi-linear dynamics away from multi-streaming regions (e.g. Nusser et al. 1991). In order to extend the applicability of this approximation beyond multi-streaming, we adopt the following scheme. Particles initially move in straight lines according to Zel’dovich, but they are merged together when they come within a critical distance of each other. This merging (sticking) produces an object with mass and linear momentum equal the total of its components. The critical distance is taken to depend on time like a diffusion length, as inspired by the adhesion approximation. This is known as the punctuated Zel’dovich (PZ) approximation (Fontana et al. 1995). This approximation is ideal for our purposes as it does not incorporate highly nonlinear effects and also it is fast and easy to implement. Further, it readily provides merging trees for individual objects.

The outline of the paper is as follows. In §2 we discuss the Zel’dovich approximation and our implementation of the punctuated Zel’dovich (PZ) scheme to describe the evolution in the quasi-linear regime. In §3 we present the PZ simulations and compare then with results from full dynamics. Our main results for halo biasing in the PZ simulations are presented in §4. We conclude with a general discussion in §5

2 THE APPROXIMATE DYNAMICS

According to the Zel’dovich approximation, the time dependent position, \mathbf{x} , of a particle with initial (Lagrangian) coordinate \mathbf{q} is

$$\mathbf{x} = \mathbf{q} + D(t)\boldsymbol{\theta}(\mathbf{q}), \quad (1)$$

where we work with comoving coordinates, the function $D(t)$ is the gravitational growth rate of linear density fluctuations, and $\boldsymbol{\theta}(\mathbf{q})$ is a vector field which is a function of \mathbf{q} only and is assumed to be derived from a potential. The physical peculiar velocity is $\mathbf{v} = a(t)d\mathbf{x}/dt = a\dot{D}\boldsymbol{\theta}$, where $a(t)$ is the expansion factor of the cosmological background. The relation (1) yields a reasonable description of the gravitational evolution in the quasi-linear regime (e.g. Nusser et al. 1991; Weinberg & Gunn 1990), but fails near collapsed regions where multi-streaming occurs. The punctuated Zel’dovich (PZ) approximation is an extension of (1), which prevents the coasting away of particles in collapsed regions and yet preserves the simplicity of the Zel’dovich kinematics. In the PZ, one starts with equal mass particles located at a uniform cubic grid at some initial time $t_i \rightarrow 0$. A particle is displaced from an initial position, \mathbf{q} , at t_i , according to (1) until it comes within a distance of d_c of another particle. The two particles are then merged together to form an “object” having their total mass and linear momentum, and placed at their center of mass. The newly formed object is then

moved according to the Zel'dovich relation (1) with θ determined from momentum conservation. The scheme is applied to describe the further merging and evolution of objects (and particles).

We interpret the PZ in the framework of the adhesion approximation according to which (e.g. Shandarin 1991, Nusser & Dekel 1990)

$$\frac{d\theta}{dD} = \nu \Delta \theta. \quad (2)$$

The viscous term modifies the Zel'dovich ansatz $\theta = \text{constant}$ in regions with high velocity gradients and prevents orbit crossing. Viscosity affects the flow over (comoving) scales $\lesssim \sqrt{D\nu}$. Above these scales the flow is described by the usual Zel'dovich approximation. For $d_c \propto \sqrt{\nu D(t)}$, the PZ is reminiscent of the adhesion approximation except that it ignores the details of the flow on scale $\lesssim \sqrt{D\nu}$ by coalescing objects which are within a distance d_c of each other. Here we work with $d_c = \sqrt{\nu D}$, as motivated by the adhesion approximation.

3 THE SIMULATIONS

We have run 60 PZ simulations, each with 512^3 equal mass particles in a $128h^{-1}\text{Mpc}$ cubic box on the side. The initial conditions correspond to a random Gaussian realization of the Cold Dark Matter scenario in a flat universe without a cosmological constant. Thus the particle mass is $4.3 \times 10^9 h^{-1} M_\odot$. The dimensionless value of the Hubble constant is $h = 0.73$ and the *rms* value of the initial mass fluctuation in a sphere of $8h^{-1}\text{Mpc}$, as extrapolated to current time, is $\sigma_8 = 0.8$. The particles are moved forward in time from $z = 1000$ to $z = 0$ according to the PZ approximation with $d_c = \sqrt{\nu D}$ with $\nu = 1h^{-2}\text{Mpc}^2$ which sets a spatial resolution of $1h^{-1}\text{Mpc}$ at the present time ($D = 1$). To further improve performance of the PZ, we smooth the initial velocity and density fields with a Gaussian window of width equal to $\sigma = 1h^{-1}\text{Mpc}$.

Our time variable is the growth factor D and the time-step, dD , is such that $|\theta_{\text{max}}|dD = 0.1d_c$, where θ_{max} is the speed of the fastest object.

For purposes of history tracking, each object is assigned a unique ID. When objects merge, the newly formed objects inherits the ID of the most massive progenitor. Object histories are tabulated in time slices separated by $\delta D = 1/100$.

At the final time, the average number of objects per simulation is 7×10^5 with 10^5 being more massive than $4.3 \times 10^{11} h^{-1} M_\odot$ which is the minimal halo mass we consider for the study of assembly bias. The number of halos in all 60 simulations is comparable to that in the millennium simulation.

The PZ approximation is neither expected nor intended to model highly non-linear dynamics. Indeed, it is because it misses highly non-linear effects that we use it in this study. However, it is prudent to make a general comparison of our implementation of the PZ scheme with results from full dynamics. To make a direct comparison, we have run the PZ scheme and a Particle-Mesh (Bertschinger & Gelb 1991) N-body code on the same initial conditions for 256^3 particles in cubic box of $64h^{-1}\text{Mpc}$ on the side. The initial conditions correspond to a flat CDM universe without a cosmological

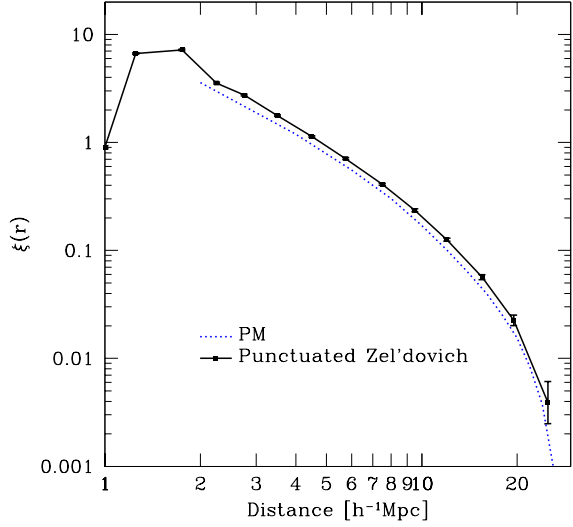


Figure 2. Density correlation functions computed from the PZ and PM simulations, as indicated in the figure. The mean of correlation functions from 60 PZ runs (each of 512^3 particles in a box of $128h^{-1}\text{Mpc}$ on the side) is shown as the solid line. The attached error-bars are 1σ . For this comparison we use a PM simulation of 256^3 particles in a box size of $512h^{-1}\text{Mpc}$ on the side.

constant and $\sigma_8 = 0.8$. Figure (1) offers a visual impression of the difference between the final results from the PZ (panels to the right) and PM simulations (to the left). In the top panels the final distribution of objects in the PZ approximation is seen to follow closely the particle distribution in the PM code. This impression is further confirmed by the contour maps of the density fields in the bottom panels. The general agreement is impressive. The density fluctuations in the PZ are slightly of larger amplitude but this maybe due to cosmic variance. In figure (2) we also plot the density correlation functions obtained from PZ runs and a PM simulation. The solid line is the mean correlation computed from the mean of 60 PZ runs (each of 512^3 particles in a box of $128h^{-1}\text{Mpc}$ on the side), while the dashed is computed from the output of a single PM simulation of 256^3 particles in a box of $512h^{-1}\text{Mpc}$ on the side. The 1σ error-bars attached to the PZ curve are estimated using the bootstrap method as follows. We generate 500 sets of simulations where each set contains 60 simulations picked randomly out of the 60 original simulations (i.e. some of these simulations could be selected more than once). For each set we compute the mean correlation and the errors are estimated as the standard deviations between the mean correlations of the 500 sets.

Objects (“halos”) in a PZ simulation are point-like and are identified using different criteria than halos in full N-body simulations. Therefore, we expect only a rough agreement between the mass functions of halos (number density versus mass) computed from PZ simulations and full dynamics. We compared the abundance of objects versus mass in the PZ runs with the analytic predictions of Sheth & Tormen (2002) and Press & Schechter (1974) for the halo mass function. The transfer function used in these predictions is taken from Bardeen et al. (1986) with a slope of $n = 1$ for the primordial power spectrum.

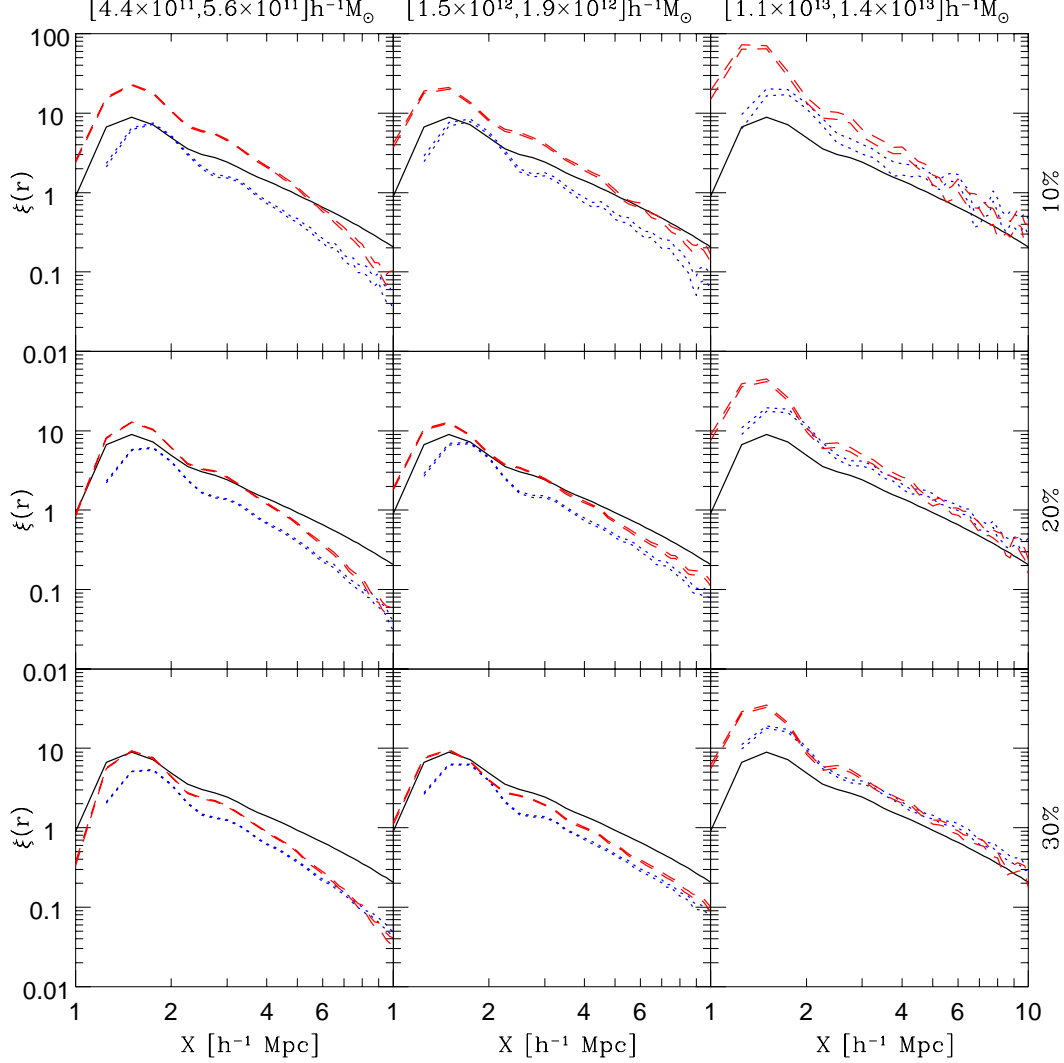


Figure 3. Correlation functions for 10%, 20% and 30% oldest/youngest halos. In each panel, the correlations are represented by curves corresponding to $\pm\sigma$ deviations. Dashed and dotted lines are for old and young halos, respectively. For comparison, the solid line in each panel shows the correlation function of the underlying mass-density.

Overall, there is only a qualitative agreement between PZ and the analytic expressions. For masses $4.3 \times 10^{11} h^{-1} M_{\odot}$ the PZ simulation agrees with PS and ST. However, for more massive halos, the PZ overestimates abundance up to a factor of two for masses $10^{13} h^{-1} M_{\odot}$. The difference is reduced as we go to higher masses until it disappears at $6 \times 10^{13} h^{-1} M_{\odot}$. At higher masses, PZ falls short of the analytic expressions by a factor which increases with mass.

4 RESULTS

The merging history of an object (“halo”) in our implementation of the PZ approximation is readily provided. We consider only halos containing more than 100 particles ($4.3 \times 10^{11} h^{-1} M_{\odot}$) at the final time ($z = 0$) and define the formation time of a halo as the redshift at which it has acquired half of its final mass (Gao, Springel & White 2005). We use the correlation functions to probe the clus-

tering properties of halos. In figure 3 we plot the correlation functions, $\xi(x)$, as a function of separation, x , for halos in three mass ranges in the left, middle and right columns, respectively. The dashed (dotted) lines in the top, middle and bottom panels, respectively, correspond to 10%, 20% and 30% oldest (youngest) halos. The solid lines in all panels are identical and represent the correlation function of the mass density field. In each panel the halo correlations are shown by two curves representing $\pm\sigma$ deviations computed using the bootstrap method, as outlined in §3. The dependence of the correlation function on the formation time is clear for all mass ranges shown in the figure. The bias persists even between the 30% youngest and 30% oldest halos.

We use the difference between the correlation functions of old and young halos to quantify the assembly bias at various separations. We determine the bias parameter b in separation range $(x, x + \Delta x)$ by minimizing the quantity (Gao, Springel & White 2007)

$$\int_{\Delta x} dx [\log \xi_{\text{old}} - \log(b^2 \times \xi_{\text{young}})]^2.$$

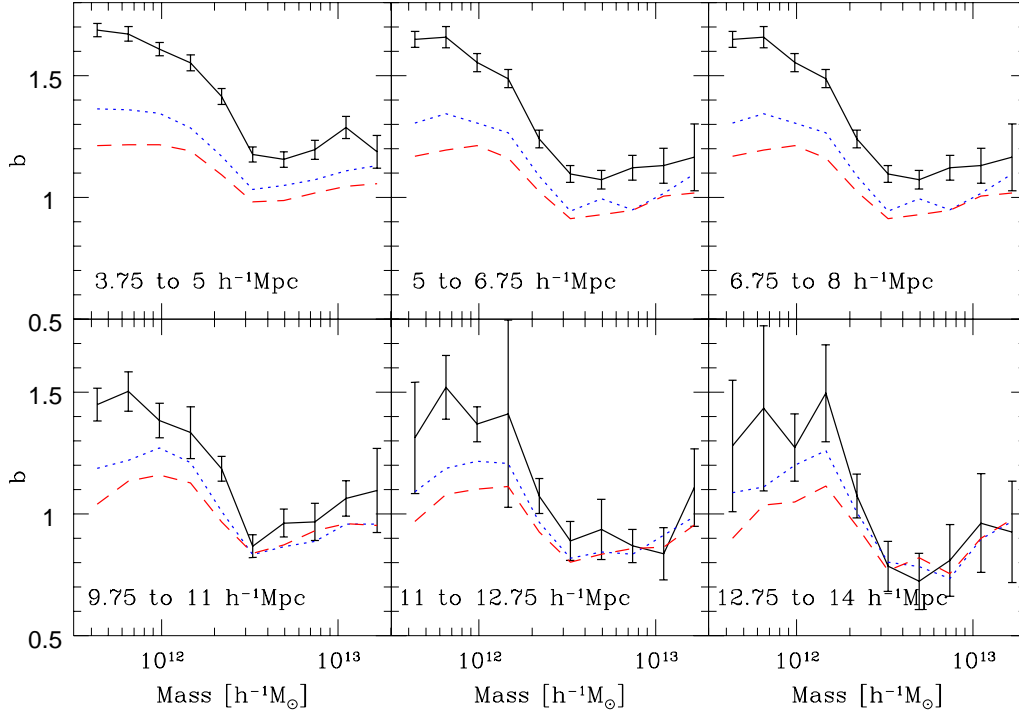


Figure 4. Square root ratio of clustering amplitude of old to young halos as a function of their mass at various separations, as indicated in the panels. Solid, dotted and dashed curves, respectively, correspond to 10%, 20% and 30% oldest/youngest haloes. Error-bars (1σ) are plotted only for the solid lines.

Figure (4) shows the bias as a function of halo mass, for various separations. For masses $\lesssim 2 \times 10^{12} M_\odot$, the bias is about 1.7 and is similar for all separations considered here. The error-bars are large at separations $> 10 h^{-1} \text{Mpc}$ and we cannot detect and increase in the bias as claimed by Gao, Springel & White (2005). The bias weakens with increasing halo mass, but remains statistically significant only for the 10% old/young halos, at separations $\lesssim 8 h^{-1} \text{Mpc}$.

Assembly bias may be caused by different environments of old and young halos. We show here that halo ages are strongly correlated with the “dimensionality” of initial fluctuation field as defined by

$$\eta \equiv \frac{\lambda_1 + \lambda_2 + \lambda_3}{\sqrt{\lambda_1^2 + \lambda_2^2 + \lambda_3^2}} \quad (3)$$

where λ_i are the eigenvalues of the tensor $\partial\theta_i/\partial q_m$. At the centers of spherical, cylindrical and planar perturbations η obtains the values $\eta = \sqrt{3}$, $\sqrt{2}$ and $\eta = 1$, respectively. We have computed the mean value η as a function of distance from particles making up young and old halos. The results are plotted in figure Fig. 5. We find that young haloes have an average higher dimensionality than old haloes.

5 CONCLUSIONS

We have shown that assembly bias of halos persists even in a simplified description of gravitational dynamics like the punctuated Zel’dovich (PZ) approximation. The PZ approximation prevents the coasting away of particles in multi-streaming regions by coalescing objects that have come

within a critical distance of each other. The PZ is fast, simple to implement, and readily provides object merging trees. This allows us to study assembly bias in a large number of simulations (60 simulations, each of 512^3 particles in a $(128 h^{-1} \text{Mpc})^3$ cubic box). The magnitude of the bias is comparable to that found in full simulations. This implies that highly non-linear effects such as mass loss from halos in the vicinity of larger mass concentrations, may not be the dominant driver for assembly bias. We intend to apply the PZ scheme to the initial conditions used in the millennium simulation (Springel et al. 2005) and compare the associated assembly bias with the result of Gao, Springel & White (2005). This will yield a better quantitative assessment of the role of highly non-linear effects.

We have found a strong correlation between halo ages and the dimensionality of the nearby initial configuration. Young halos tend to form in regions of higher initial dimensionality than old halos. This is explained by the dependence of collapse time on dimensionality- a spherical perturbation collapses slower than a planar perturbation with the same initial density (Bertschinger & Jain 1994). Therefore, assembly bias would be explained if one could show that regions of lower dimensionality are more correlated than those of higher dimensionality.

ACKNOWLEDGMENT

This research is funded by the German-Israeli Foundation for Scientific Research and Development. We thank Vincent

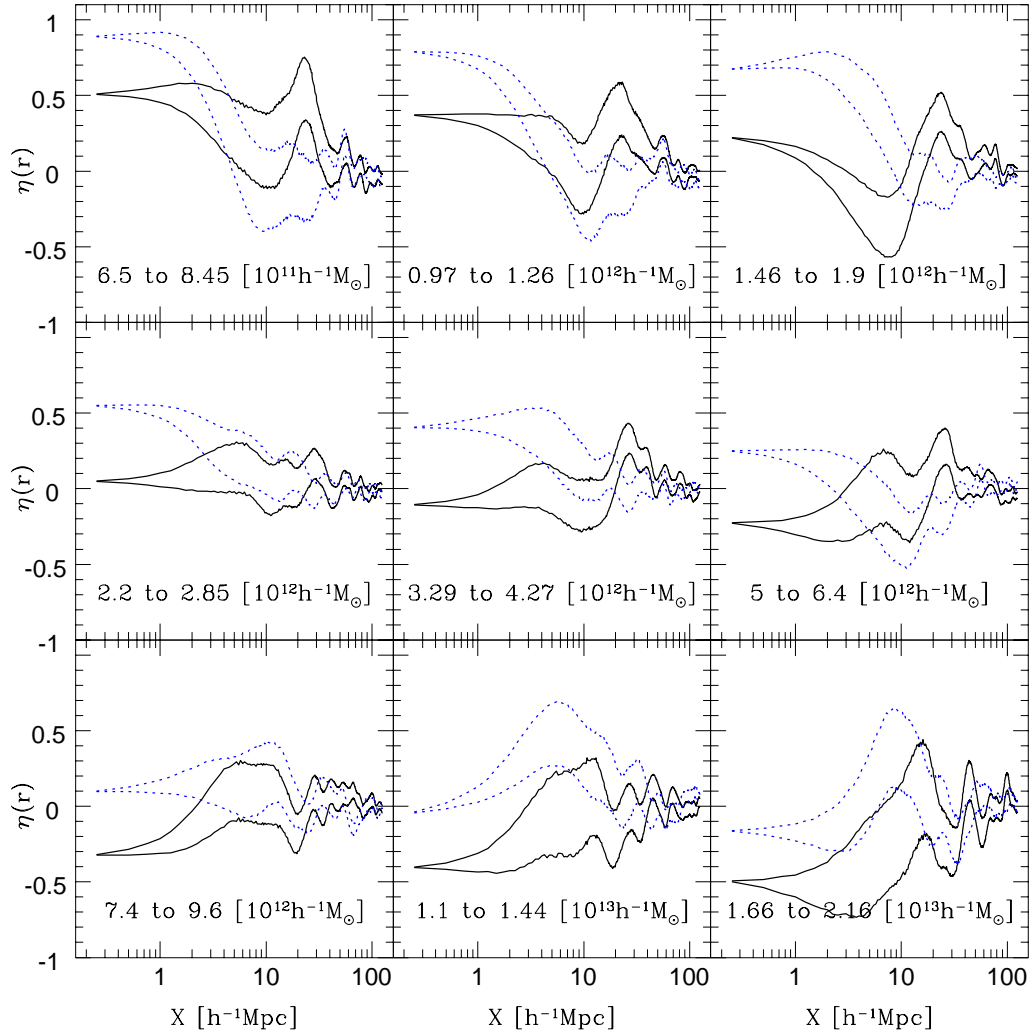


Figure 5. The mean dimensionality parameter, η , as a function of separation from particles making up young (dotted blue lines representing $\pm\sigma$ deviations from the mean) and old haloes (solid black lines), all for 10% oldest/youngest haloes.

Desjacques for stimulating discussions and Liron Gleser for help with the simulations and data analysis.

REFERENCES

- Bardeen J.M., Bond J. R., Kaiser N. & Szalay A.S., 1986, *ApJ*, 304, 15
- Bertschinger E. & Gelb J. M., 1991, *Computers in Physics*, 5, 164
- Bertschinger E., Jain B., 1994, *ApJ*, 431, 486
- Bond J. R., Cole S., Efstathiou G., Kaiser N., 1991, *ApJ*, 379, 440
- Diemand J., Kuhlen M. & Madau P., 2007, *arXiv:astro-ph/0703337v2*
- Fontana L., Millesi M., Murante G. & Provenzale A., 1995, *Il Nuovo Cimento C*, 18, 5, 531
- Gao L., Springel V., White S. D. M., 2005, *MNRAS*, 363, 66
- Gao L., Springel V., White S. D. M., 2007, *MNRAS*, 377, L5
- Harker G., Cole S., Helly J., Frenk, C. & Jenkins A. 2006, *MNRAS*, 367, 1039
- Jing Y. P., Suto Y. & Mo H. J., 2007, *ApJ*, 657, 664
- Lacey C., Cole S., 1993, *MNRAS*, 262, 627
- Lemson G., Kauffmann G., 1999, *MNRAS*, 302, 111
- Mo H. J. White S. D. M., 1996, *MNRAS*, 282, 347
- Nusser A., Dekel A., Bertschinger E. & Blumenthal G. R., 1991, *ApJ*, 379, 6
- Nusser A. & Dekel A., 1990, *ApJ*, 362, 14
- Percival W. J., Scott D., Peacock J. A., Dunlop J. S., 2003, *MNRAS*, 338, 31L
- Press W. H. & Schechter P., 1974, *ApJ*, 187, 425
- Risa H. W., Andrew R. Z., James S. B., Andrey V. K. & Brandon A., 2006, *ApJ*, 652, 71
- Shandarin S., 1991, *Astronomical Society of the Pacific Conference Series*, 15, 189
- Sandvik H. B., Möller O., Lee J. & White S. D. M., 2007, *MNRAS*, 377, 234
- Sandvik H. B., Möller O., Lee J. & White S. D. M., 2005, *MNRAS*, 363, 66
- Sheth R. K., Tormen G., 2004, *MNRAS*, 350, 1385
- Sheth R. K., Tormen G., 2002, *MNRAS*, 329, 61
- Springel V. et al. , 2005, *Nature*, 435, 629
- Wang H. Y., Mo H. J. & Jing Y. P., 2007, *MNRAS*, 375, 633
- Wechsler R. H., Zentner A. R., Bullock J. S., Kravtsov A. V., Allgood B., 2006, *ApJ*, 652, 71
- Wechsler R. H., Bullock J. S., Primack J. R., Kravtsov A. V. & Dekel, A., 2002, *ApJ*, 568, 52

- Weinberg D. H. & Gunn E. J., 1990, MNRAS, 247, 260
White S. D. M., 1996, in Schaeffer R., Silk J., Spiro M., Zinn
Justin J., eds, Cosmology and Large Structure, Les Houches
Session LX. Elsevier, Amsterdam, P.77 s 379, 440